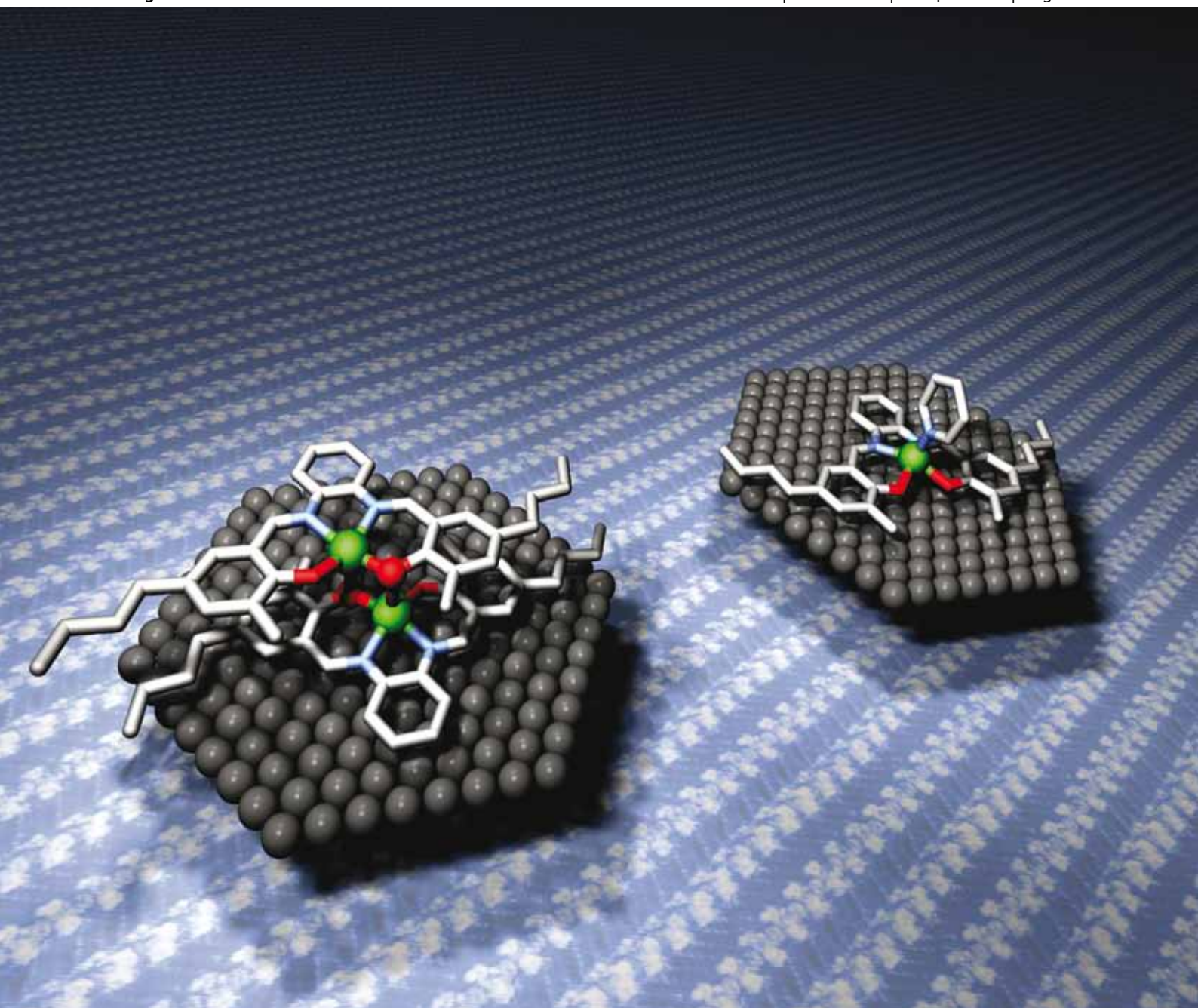


ChemComm

Chemical Communications

www.rsc.org/chemcomm

Volume 46 | Number 15 | 21 April 2010 | Pages 2513–2692



ISSN 1359-7345

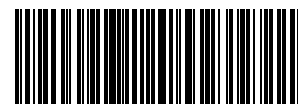
RSC Publishing

COMMUNICATION

Johannes A. A. W. Elemans *et al.*
Axial ligand control over monolayer
and bilayer formation of metal-
salophens at the liquid–solid interface

FEATURE ARTICLE

Bjorn ter Horst, Ben L. Feringa and
Adriaan J. Minnaard
Iterative strategies for the synthesis of
deoxypropionates



1359-7345(2010)46:15;1-K

Axial ligand control over monolayer and bilayer formation of metal-salophens at the liquid–solid interface†‡

Johannes A. A. W. Elemans,^{*a} Sander J. Wezenberg,^b Michiel J. J. Coenen,^c Eduardo C. Escudero-Adán,^b Jordi Benet-Buchholz,^b Duncan den Boer,^c Sylvia Speller,^c Arjan W. Kleijj^{*bd} and Steven De Feyter^{*a}

Received (in Cambridge, UK) 23rd October 2009, Accepted 7th January 2010

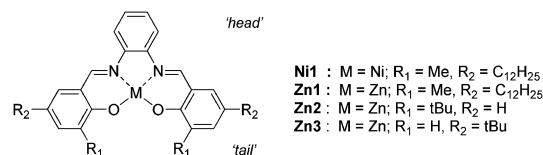
First published as an Advance Article on the web 25th January 2010

DOI: 10.1039/b922212j

Nickel salophens exclusively form monolayers at a liquid–solid interface, while in contrast zinc salophens mainly self-assemble into bilayers via axial ligand self-coordination which can be disrupted by the addition of pyridine axial ligands.

One of the most exciting topics nowadays in scanning tunneling microscopy (STM) research is the imaging of dynamic processes, such as host–guest complexation¹ and reactivity² of functional molecules self-assembled at a liquid–solid interface. In particular metal-porphyrins represent versatile platforms for the single molecule imaging of axial ligand coordination³ and catalytic processes⁴ at their reactive metal centre. Also metal-salophens are interesting molecules for such studies since their flat structure is ideal for adsorption at a surface. Their rich coordination behaviour⁵ and the wealth of reactions they can catalyse,⁶ depending on the metal centre, make them promising candidates to reveal their structure and function at the single molecule level with STM. It is therefore surprising that so far only a limited number of STM studies have been reported on metal-salen complexes.⁷ Here we present our investigations on the metallosupramolecular behaviour and function of metal-salophens **Ni1** and **Zn1** at the liquid–solid interface with STM.⁸ Nickel salens have been reported as catalysts for oxidation reactions,⁹ while zinc salens can catalyse the alkynylation of ketones.¹⁰ We will show that **Ni1** exclusively forms monolayers, while **Zn1** can dimerise via axial ligand self-coordination. The latter leads to the formation of bilayers, and this bilayer formation can be reversed in a

controlled fashion by the addition of external axial pyridine ligands.



Immediately after depositing a droplet of a 1 mM solution of **Ni1** or **Zn1** in 1-phenyloctane onto a piece of freshly cleaved highly oriented pyrolytic graphite (HOPG), extended two-dimensional layers of lamellar arrays of these compounds were observed by STM. The lamellar periodicity is 2.4 ± 0.1 nm, and in individual lamellae of **Ni1** the molecules are generally arranged in a head-to-tail geometry at a distance of 1.2 nm, with the 1,2-diminobenzene moieties located in the centre (Fig. 1 and ESI†). Rather frequently, within the lamellae defects are present where the orientation direction of the salophen cores is switched 180 degrees, with a tail-to-tail dimer of **Ni1** as the switching point (see Fig. 1a). The head-to-tail arrangement of molecules of **Ni1** in adjacent lamellae is either aligned, or oppositely directed (ESI†). Due to this randomness no general unit cell could be assigned. Within a single domain the alkyl chains of **Ni1** are all interdigitated and directed along one of the main symmetry axes of graphite, irrespective of the orientation direction of the salophen cores.

The self-assembly behaviour of **Zn1** at the same liquid–solid interface is strikingly different from that of **Ni1**. Instead of homogeneous domains of well-resolved molecules, the majority of the surface was covered with less ordered and less

^a Department of Chemistry, Division of Molecular and Nano Materials, and INPAC – Institute for Nanoscale Physics and Chemistry, Katholieke Universiteit Leuven, Celestijnenlaan 200-F, 3001 Leuven, Belgium. E-mail: J.Elemans@science.ru.nl, steven.defeyter@chem.kuleuven.be

^b Institute of Chemical Research of Catalonia (ICIQ), Av. Països Catalans 16, 43007 Tarragona, Spain. E-mail: akleijj@iciq.es

^c Institute for Molecules and Materials, Radboud University Nijmegen, Heyendaalseweg 135, 6525 AJ Nijmegen, The Netherlands

^d Institució Catalana de Recerca i Estudis Avançats (ICREA), Pg. Lluís Companys 23, 08010 Barcelona, Spain

† Dedicated to Roeland J. M. Nolte and Javier de Mendoza on the occasion of their 65th birthdays.

‡ Electronic supplementary information (ESI) available: Synthetic details for **Zn1** and **Ni1**, STM procedures, magnifications of STM images and computer-modeled structures of the monolayers, statistics, additional crystallographic details, NMR and UV-vis titration data. CCDC 748345 for **Zn1-Pyr**. For ESI and crystallographic data in CIF or other electronic format see DOI: 10.1039/b922212j

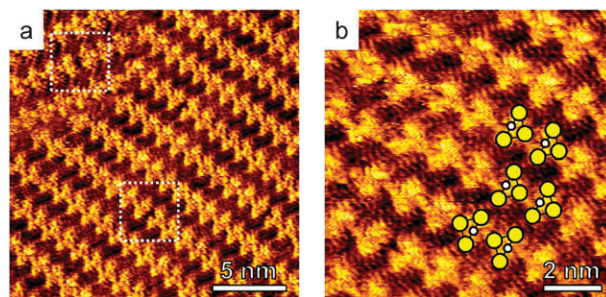


Fig. 1 (a) STM topography of a monolayer of **Ni1** at the graphite/1-phenyloctane interface; $V_{\text{bias}} = -680$ mV, $I_{\text{set}} = 417$ pA; the dashed white rectangles indicate a switch of orientation of the molecules of **Ni1** within a lamellar array. (b) Zoom with some schematic **Ni1** molecules superimposed to indicate their orientation.

well-resolved lamellar arrays, with a periodicity of 2.3 ± 0.1 nm, as observed by STM (Fig. 2a and ESI†). We conclude there is a bilayer stacking of **Zn1** molecules, composed of double-stranded lamellae of cofacially stacked metal-salophen units. In these complex structures the alkyl chains are no longer resolved. In the cross section, three distinct height levels can be discriminated (Fig. 2b). The height differences in between them measure ~ 0.25 nm. We propose that the observed heights correspond to locations in the layer where a bilayer structure of dimeric complexes of **Zn1** (D), a monolayer structure (M), and vacancies (V) are present (Fig. 2b and ESI†). Inspection of many locations on the samples yielded no indication of higher order multilayers, suggesting that the self-assembly stops at the level of a dimer.¹¹

The ability of zinc salophen complexes such as **Zn1** to form dimeric assemblies in the solid state *via* μ_2 -O bridging has been previously investigated by X-ray diffraction.¹² In the case of **Zn1**, such an axial ligand-directed self-assembly can lead to the formation of stable homodimers with a structure as shown in Fig. 2c. Cofacial homodimers, in which the two zinc centres are involved in a four-point interaction and one of the phenolic oxygen atoms of each molecule bridges in an axial-ligand fashion to its dimeric partner molecule, are believed to give a highly stable assembled state.

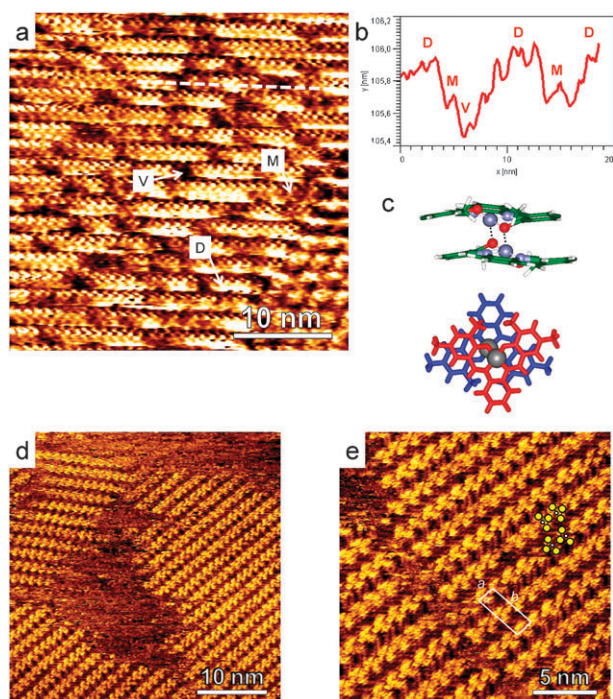


Fig. 2 (a) STM topography of a self-assembled layer of **Zn1** at the interface of graphite and 1-phenyloctane; $V_{\text{bias}} = -680$ mV, $I_{\text{set}} = 205$ pA; locations of a dimeric structure (D), a monomeric structure (M), and a vacancy (V) are indicated. (b) Cross section corresponding to the dashed white trace in (a). (c) Computer-modelled dimer of **Zn1** (side and top view), based on the STM and NMR dilution studies, showing the proposed four-point coordinative interaction (alkyl chains have been omitted). (d) STM topography image of monolayer domains of **Zn1**. (e) Zoom with the unit cell depicted; $a = (1.2 \pm 0.1)$ nm, $b = (4.1 \pm 0.2)$ nm, $\alpha = (86 \pm 2)^\circ$; some schematic molecules of **Zn1** are drawn in.

The assembly formation of **Zn1** was further examined in solution by ^1H NMR dilution experiments. In CDCl_3 , no observable changes in the proton signals were noted in the concentration range 10^{-3} – 10^{-4} M. However, the addition of 5% of CD_3OD to a 10^{-3} M solution resulted in significant downfield shifts (0.1–0.3 ppm) of all aromatic and imine proton signals of the compound, as well as the signals of the aryl- CH_3 groups and the first methylene group of the alkyl chains. In contrast, the proton signals of **Ni1** in CDCl_3 appeared to be insensitive to the addition of CD_3OD (ESI†). The NMR results are in line with the breaking up of dimeric into monomeric **Zn1** species as a result of the competitive axial coordination of CD_3OD to **Zn1**. Various examples of zinc salen derivatives to which nitrogen- or oxygen-donor ligands are axially coordinated have been reported.^{12b,13} The basis for the strong binding of these donor ligands is the high Lewis acidity of the zinc ion, which is dictated by the rigid geometry enforced by the salophen ligand.¹⁴

To quantify the dimerisation of **Zn1** in solution, UV-vis dilution measurements in toluene were carried out at concentrations as low as 10^{-6} M. No changes were noted in the UV-vis spectrum between 10^{-4} to 10^{-6} M, indicative of a strong association process. Since no direct measurement of K_{dimer} could be accomplished, the self-assembly behaviour of two different but electronically similar zinc salophen model complexes **Zn2** and **Zn3** (ESI†) was investigated. These complexes only differ in the position of the two pendent ^tBu groups. The presence of two ^tBu groups in the 3-position of the salophen ligand (**Zn2**) effectively suppresses dimer formation,^{12b,15} while for **Zn3** a dimeric species is expected to prevail in solution. From these titration studies the K_{dimer} for **Zn3** was estimated to be $3.2 \pm 0.01 \times 10^8 \text{ M}^{-1}$. This very high association constant for the dimer species further supports the observation of bilayers of **Zn1** by STM.

Although the majority of the surface ($>90\%$) was covered with a layer of predominantly dimeric species, occasionally very small domains containing exclusively well-resolved monomeric structures of **Zn1** were found (Fig. 2d–e). These domains were very unstable and typically disappeared within a couple of minutes. Lowering the concentration of **Zn1** in the subphase to 0.2 mM did not lead to large variations in the population between the monolayer and bilayer domains. In comparison with the monolayer of **Ni1**, the monolayers of **Zn1** are more homogenic in the sense that hardly any defects were found and the direction of the head-to-tail orientation of the molecules alternated with high regularity between adjacent lamellae. Remarkably, in contrast to monolayers of **Ni1**, the alkyl chains between the lamellae of **Zn1** are, while being interdigitated, organized in a zig-zag geometry, thereby still following two of the underlying graphite main symmetry axes. The lamellar periodicity is somewhat smaller, *viz.* 2.2 ± 0.1 nm.

The high regularity and in particular the complete absence of dimeric structures in the monolayer domains is in sharp contrast with the domains where the dimeric complexes prevail. It suggests that the formation of the second layer is a cooperative process, which is reflected in the complete absence, all over the sample, of single dimeric complexes or even small domains of them.

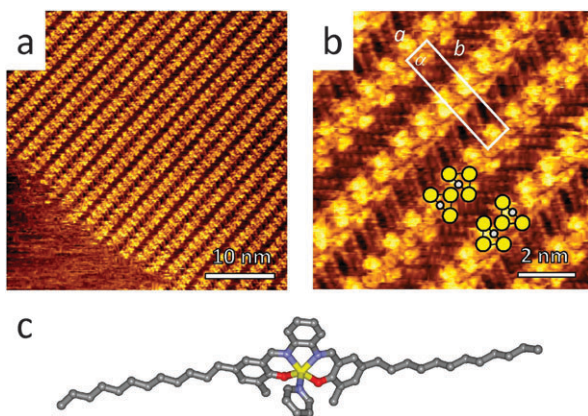


Fig. 3 (a) STM image of the interface between graphite and a solution of **Zn1** (1 mM) and pyridine (10 mM) in 1-phenyloctane. $V_{\text{bias}} = -680$ mV, $I_{\text{set}} = 221$ pA. (b) Magnification showing the unit cell; $a = (1.1 \pm 0.1)$ nm, $b = (4.3 \pm 0.2)$ nm, $\alpha = (88 \pm 2)^\circ$; some schematic salens are drawn in. (c) X-ray structure of the complex between **Zn1** and pyridine.

Since zinc salens form strong complexes with N-donor axial ligands,¹³ it was reasoned that the complexation of such a ligand to **Zn1** would inhibit dimerisation and possibly result in the formation of discrete 1 : 1 salphen-ligand complexes at the liquid–solid interface. **Zn1** was found to form a strong complex with pyridine and the X-ray structure of the 1 : 1 complex was solved, which is depicted in Fig. 3c. Indeed, when a solution of **Zn1** and 10 equiv. of pyridine in 1-phenyloctane was brought onto a graphite surface, STM revealed the complete absence of the bilayer-like features and over the entire sample homogeneous domains of lamellar arrays with high internal resolution and a periodicity of 2.3 ± 0.1 nm are observed (Fig. 3a–b). As found in the case of the monolayers of uncomplexed **Zn1**, the alkyl chains are interdigitated. Although the pyridine ligands could not be directly imaged, it is obvious that they must play a crucial role in the adsorption behaviour of **Zn1** at the liquid–solid interface. The successful competition of the pyridine ligand with a second molecule of **Zn1** for coordination at the zinc metal in solution is directly translated to the self-assembly of **Zn1** in a layer of monomers at the surface.

In summary, we have shown that metal-salophens with a high structural similarity can be imaged with high resolution in STM. The molecules self-assemble in strikingly different architectures at the liquid–solid interface, as a result of axial ligand effects. The elucidation of such structural behaviour at the single molecule level with STM can be of great importance for the reactivity of catalytic surfaces. In particular, it can be expected that different molecular organisations will give rise to differences in reactivity. Future work will be therefore directed to investigate the relationship between structure and reactivity of metal-salophens at the liquid–solid interface, studied *in situ* by STM.

The Fund of Scientific Research–Flanders (FWO), K. U. Leuven (GOA 2006/2), the Belgian Federal Science Policy Office (IAP-6/2), ICIQ, ICREA, the Spanish Ministry

of Science and Innovation (MICINN, project CTQ2008-02050/BQU) and Consolider Ingenio 2010 (grant CSD2006-0003), and NanoNed – the Dutch nanotechnology initiative by the Ministry of Economic Affairs, are acknowledged for financial support.

Notes and references

- (a) T. Kudernac, S. Lei, J. A. A. W. Elemans and S. De Feyter, *Chem. Soc. Rev.*, 2009, **38**, 402; (b) S. Stepanow, M. Lingenfelder, A. Dmitriev, H. Spillmann, E. Delvigne, N. Lin, X. Deng, C. Cai, J. V. Barth and K. Kern, *Nat. Mater.*, 2004, **3**, 229; (c) G. Schull, L. Douillard, C. Fiorini-Debuisschert, F. Charra, F. Mathevet, D. Kreher and A. J. Attias, *Nano Lett.*, 2006, **6**, 1360; (d) S. J. H. Griessl, M. Lackinger, F. Jamitzky, T. Markert, M. Hietschold and W. M. Heckl, *J. Phys. Chem. B*, 2004, **108**, 11556; (e) N. Wintjes, D. Bonifazi, F. Cheng, A. Kiebele, M. Stöhr, T. Jung, H. Spillmann and F. Diederich, *Angew. Chem., Int. Ed.*, 2007, **46**, 4089; (f) J. Adisojoso, K. Tahara, S. Okuhata, S. Lei, Y. Tobe and S. De Feyter, *Angew. Chem., Int. Ed.*, 2009, **48**, 7353.
- (a) L. Piot, D. Bonifazi and P. Samorì, *Adv. Funct. Mater.*, 2007, **17**, 3689; (b) J. A. A. W. Elemans, S. Lei and S. De Feyter, *Angew. Chem., Int. Ed.*, 2009, **48**, 7298; (c) J. A. A. W. Elemans, *Mater. Today*, 2009, **12**, 34.
- (a) J. Visser, N. Katsonis, J. Vicario and B. L. Feringa, *Langmuir*, 2009, **25**, 5980; (b) M. C. Lensen, J. A. A. W. Elemans, S. J. T. van Dingenen, J. W. Gerritsen, S. Speller, A. E. Rowan and R. J. M. Nolte, *Chem.–Eur. J.*, 2007, **13**, 7948.
- B. Hulsken, R. van Hameren, J. W. Gerritsen, T. Khoury, P. Thordarson, M. J. Crossley, A. E. Rowan, R. J. M. Nolte, J. A. A. W. Elemans and S. Speller, *Nat. Nanotechnol.*, 2007, **2**, 285.
- (a) P. G. Cozzi, *Chem. Soc. Rev.*, 2004, **33**, 410; (b) A. C. W. Leung and M. J. MacLachlan, *J. Inorg. Organomet. Polym. Mater.*, 2007, **17**, 57; (c) S. J. Wezenberg and A. W. Kleij, *Angew. Chem., Int. Ed.*, 2008, **47**, 2354; (d) A. W. Kleij, *Chem.–Eur. J.*, 2008, **14**, 10520; (e) D. A. Atwood and M. J. Harvey, *Chem. Rev.*, 2001, **101**, 37.
- (a) K. Matsumoto, B. Saito and T. Katsuki, *Chem. Commun.*, 2007, 3619; (b) E. N. Jacobsen, *Acc. Chem. Res.*, 2000, **33**, 421; (c) E. M. McGarrigle and D. G. Gilheany, *Chem. Rev.*, 2005, **105**, 1563; (d) C. Baleizão and H. Garcia, *Chem. Rev.*, 2006, **106**, 3987; (e) D. J. Darensbourg, *Chem. Rev.*, 2007, **107**, 2388.
- (a) M. T. Räisänen, F. Mögele, S. Feodorow, B. Rieger, U. Ziener, M. Leskelä and T. Repo, *Eur. J. Inorg. Chem.*, 2007, 4028; (b) S. Kuck, S.-H. Chang, J.-P. Klöckner, M. H. Prosenc, G. Hoffmann and R. Wiesendanger, *ChemPhysChem*, 2009, **10**, 2008.
- For a review on STM of metallosupramolecular systems see: S.-S. Li, B. H. Northrop, Q.-H. Yuan, L.-J. Wan and P. J. Stang, *Acc. Chem. Res.*, 2009, **42**, 249.
- R. Ferreira, H. Garcia, B. de Castro and C. Freire, *Eur. J. Inorg. Chem.*, 2005, 4272.
- P. G. Cozzi, *Angew. Chem., Int. Ed.*, 2003, **42**, 2895.
- Some other examples of multilayered structures visualised by STM: (a) L. Piot, C. Marie, X. Feng, K. Müllen and D. Fichou, *Adv. Mater.*, 2008, **20**, 3854; (b) S. Lei, J. Puigmarti-Luis, A. Minoia, M. Van der Auweraer, C. Rovira, R. Lazzaroni, D. B. Amabilino and S. De Feyter, *Chem. Commun.*, 2008, 703.
- (a) J. Reglinski, S. Morris and D. Stevenson, *Polyhedron*, 2002, **21**, 2175; (b) A. W. Kleij, M. Kuil, M. Lutz, D. M. Tooke, A. L. Spek, P. C. J. Kamer, P. W. N. M. van Leeuwen and J. N. H. Reek, *Inorg. Chim. Acta*, 2006, **359**, 1807.
- (a) E. C. Escudero-Adán, J. Benet-Buchholz and A. W. Kleij, *Eur. J. Inorg. Chem.*, 2009, 3562; (b) E. C. Escudero-Adán, J. Benet-Buchholz and A. W. Kleij, *Inorg. Chem.*, 2008, **47**, 4256; (c) E. C. Escudero-Adán, J. Benet-Buchholz and A. W. Kleij, *Inorg. Chem.*, 2008, **47**, 410.
- A. W. Kleij, D. M. Tooke, M. Kuil, M. Lutz, A. L. Spek and J. N. H. Reek, *Chem.–Eur. J.*, 2005, **11**, 4743.
- A. L. Singer and D. A. Atwood, *Inorg. Chim. Acta*, 1998, **277**, 157.